Why Do Many C_2-Symmetric Bisphosphine Ligands Fail in Asymmetric Hydroformylation? Theory in Front of Experiment

Dieter Gleich and Wolfgang A. Herrmann*

Anorganisch-chemisches Institut, Technische Universität München, Lichtenbergstrasse 4, D-85747 Garching, Germany

Received May 24, 1999

Supported by a pure QM and MM treatment, stereoselectivities of rhodium systems containing the C_2-symmetric ligands CHIRAPHOS (2,3-bis(diphenylphosphino)butane; **2**), BINAP (2,2′-bis(diphenylphosphino)-1,1′-binaphthyl; **3**), DIOP (2,2-dimethyl-4,5-bis((diphenylphosphino)methyl)-1,3-dioxolane; **4**), and NAPHOS (2,2′-bis((diphenylphosphino)methyl)-1,1′-binaphthyl; **5**) have been calculated with a combined QM/MM method. On the basis of the RSAI (requirement of synchronous asymmetric inductions), which states that all ligand coordination modes favor transition states with the same asymmetric induction, we demonstrate that the performance of C_2-symmetric bidentate phosphine ligands is governed by two interdependencies, namely induction influence of the chelate ring and backbone flexibility. In a further step, the NAPHOS derivatives **6** (2,2′-bis((2-dinaphthylphosphino)-methyl)-1,1′-binaphthyl) and **7** (2,2′-bis((1-dinaphthylphosphino)methyl)-1,1′-binaphthyl) which to our knowledge have not been tested experimentally up to now, have been investigated in the same manner. **7** fulfills the RSAI and will be tested experimentally. Our explanations and predictions release asymmetric hydroformylation from its predominantly empirical character, although the magic formula for ligand development is still unknown.

Introduction

Hydroformylation,[1] the largest scale process of homogeneous organometallic catalysis,[2] would gain even more attraction if stereoselective routes to a number of key chemicals were available.[3] The sum reaction (Scheme 1) offers, besides the general demand for high chemoselectivities, two fundamental issues: (i) regioselectivity $S_{n/iso}$, the ratio of linear to branched aldehyde (*n*:*iso*), and (ii) stereoselectivity, the enantiomeric excess (ee) of one chiral *iso*-aldehyde.

In asymmetric hydroformylation, bimetallic platinum−tin systems are more prone to the hydrogenation side reaction than rhodium catalysts, which, however, achieve only low ee's.[3] The asymmetric induction springs from interactions of the substrates with chiral, mostly bidentate ligands—usually bisphosphines, bisphosphites, or species with mixed functionalities.[3]

Nearly all of these ligands have been used with both metals,[3] and the corresponding catalysts are often successful in asymmetric hydrogenation but not in hydroformylation. In certain cases, low ee's of platinum are opposed to those of rhodium systems, or a distinct higher-to-lower divergence going from platinum to rhodium is observed. Nevertheless, since the origin of stereodifferentiation, namely olefin insertion, is identical, the question arises if some general ligand features control the hydroformylation stereoselectivity. The goal is not only to explain the behavior of established catalysts but also to predict the performance of new ligands.

Scheme 1

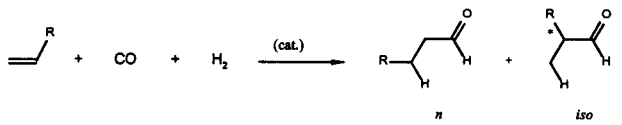

In two previous papers we have outlined a combined QM/MM method with frozen reaction centers in challenges of stereoselective and regioselective rhodium-catalyzed hydroformylation.[4] The essential difference of our semiquantitative theoretical approach as compared to the qualitative model of Pino and Consiglio[5] lies in the explicit consideration of all relevant transition-state geometries. Supported by experiment,[1,6] two assumptions have been made: (i) both the regio- and stereoselectivity of hydroformylation are exclusively determined during olefin insertion, and (ii) this step is irreversible.

* To whom correspondence should be addressed. E-mail: lit@arthur.anorg.chemie.tu-muenchen.de.

(1) Reviews: (a) Herrmann, W. A.; Cornils, B. *Angew. Chem., Int. Ed. Engl.* **1997**, *36*, 1047. (b) Cornils, B.; Herrmann, W. A. In *Applied Homogeneous Catalysis with Organometallic Compounds*; VCH-Wiley: Weinheim, Germany, 1996; Vol. 1, pp 3−25. (c) Cornils, B.; Herrmann, W. A.; Rasch, M. *Angew. Chem., Int. Ed. Engl.* **1994**, *33*, 2144.

(2) (a) Frohning, C. D.; Kohlpaintner, C. W. In *Applied Homogeneous Catalysis with Organometallic Compounds*; VCH-Wiley: Weinheim, Germany, 1996; Vol. 1, pp 29−104. (b) Herrmann, W. A.; Kohlpaintner, C. W. *Angew. Chem., Int. Ed. Engl.* **1993**, *32*, 1524.

(3) Reviews: (a) Agbossou, F.; Carpentier, J.-F.; Mortreux, A. *Chem. Rev.* **1995**, 2485. (b) Gladiali, S.; Bayon, J. C.; Claver, C. *Tetrahedron: Asymmetry* **1995**, *6*, 1453.

(4) (a) Gleich, D.; Schmid, R.; Herrmann, W. A. *Organometallics* **1998**, *17*, 2141. (b) Gleich, D.; Schmid, R.; Herrmann, W. A. *Organometallics* **1998**, *17*, 4828.

(5) Consiglio, G.; Pino, P. *Top. Curr. Chem.* **1982**, *105*, 77.

(6) Casey, C. P.; Petrovich, L. M. *J. Am. Chem. Soc.* **1995**, *117*, 6007.

10.1021/om990393e CCC: $18.00
Publication on Web 09/21/1999

Chart 1

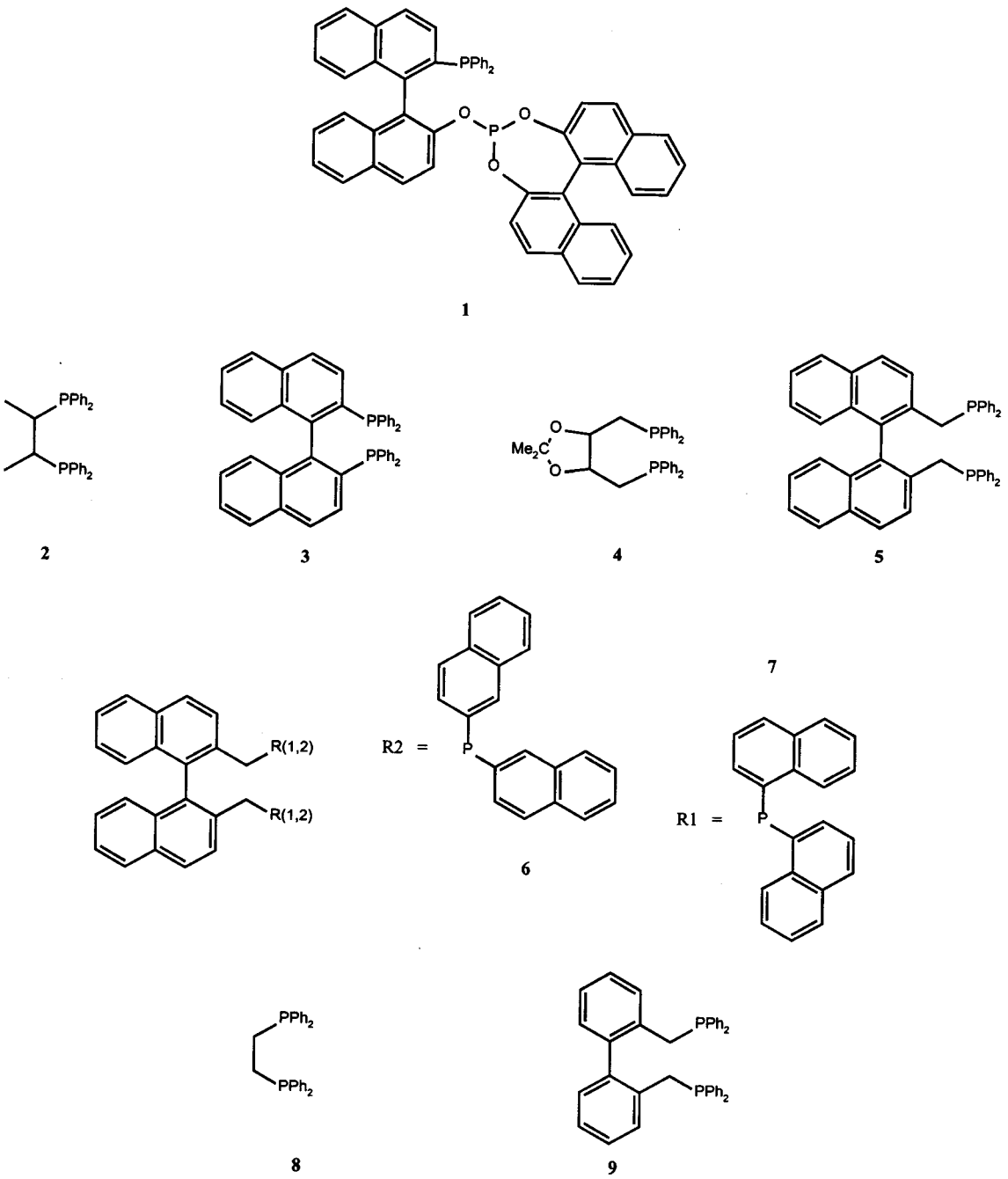

Only the relative energies of the transition states of olefin insertion must then be found to calculate the selectivities.[4−6] Furthermore, an isolated molecule in the gas phase is considered; i.e., solvent effects are neglected.[4] The substrate of choice is styrene because it acts as a common model compound in asymmetric hydroformylation.[3] After elucidating the principle that accounts for the outstanding properties of the C_1-symmetric phosphine−phosphite ligand BINAPHOS (((2-diphenylphosphino)-1,1′-binaphthalene-2′-yl) (1,1′-binaphthalene-2,2′-diyl) phosphite; **1**),[4a,7] we focus in the present paper on the six C_2-symmetric bisphosphine ligands **2**−**7** (Chart 1).

CHIRAPHOS (2,3-bis(diphenylphosphino)butane; **2**),[8] BINAP (2,2′-bis(diphenylphosphino)-1,1′-binaphthyl; **3**),[9] DIOP (2,2-dimethyl-4,5-bis((diphenylphosphino)methyl)-1,3-dioxolane; **4**),[10] and NAPHOS (2,2′-bis((diphenylphosphino)methyl)-1,1′-binaphthyl; **5**)[11] mark important stages in the development of stereoselective hydrogenation and hydroformylation catalysts, respectively. The chirality of these ligands is introduced in two ways: for **2** and **4**, an achiral backbone has been modified by substituents (**2** is related to DIPHOS (1,2-bis(diphenylphosphino)-ethane; **8**[4b]), whereas for **3** and **5**, the backbone itself is of axial chirality (**5** is the naphthyl analogue of BISBI (2,2′-bis((diphenylphosphino)methyl)-1,1′-biphenyl; **9**[4b])). The ring size increases from **2** to **5** and ensures a further

(7) Nozaki, K.; Sakai, N.; Nanno, T.; Higashijima, T.; Mano, S.; Horiuchi, T.; Takaya, H. *J. Am. Chem. Soc.* **1997**, *119*, 4413.

(8) Fryzuk, M. D.; Bosnich, B. *J. Am. Chem. Soc.* **1977**, *99*, 6262.

(9) Noyori, R. *Asymmetric Catalysis in Organic Synthesis*; Wiley: New York, 1994; Chapter 2.

(10) Kagan, H. B.; Dang, T. P. *J. Am. Chem. Soc.* **1972**, *94*, 6429.

(11) Herrmann, W. A.; Kohlpaintner, C. W.; Herdtweck, E.; Kiprof, P. *Inorg. Chem.* **1991**, *30*, 4271.

Chart 2

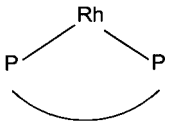

variation. **6** (2,2′-bis((2-dinaphthylphosphino)methyl)-1,1′-binaphthyl) and **7** (2,2′-bis((1-dinaphthylphosphino)methyl)-1,1′-binaphthyl) are NAPHOS derivatives with greater steric demand of the phosphorus substituents. To our knowledge, they have not been tested experimentally up to now.

Computational Methods

a. Relative Energies of Coordination Modes. For all DFT calculations, the DZVP basis set[12] was chosen. Further details about this basis set have already been discussed elsewhere.[13a] All structures were optimized without any restrictions on the LDA or NLDA (BP86) level of theory.[14,15] In the first case, total energies were calculated by NLDA single-point calculations using the LDA geometry. If not mentioned explicitly, the resulting geometries were verified to be true minima or first-order transition states by analytical calculation of the second energy derivative matrix. All calculations were performed with the programs DGauss[16,17a] (UniChem Interface[17b]) and Gaussian98.[18]

b. Bite-Angle Calculations. The natural bite angle concept[19,20] was modified in the following way: metal−ligand fragments (Chart 2) with fixed Rh−P bond lengths and zero P−Rh−P bending force constants were subject to one 100 ps gas-phase MD simulation at constant high temperature (1000 K). Every 1 ps the structures were minimized, and the bite angle from the lowest energy structure was taken as the preferred bite angle (PBA). Additionally, the bite angle and energy range of all stable structures was determined.

The calculations were performed with the cff91 force field[21] extended by phosphorus parameters[22] (force field version F,[4b] see below) and the Insight/Discover program package.[23]

c. Transition-State and ee Calculations. Fundamental aspects have already been discussed elsewhere.[4,13b] It must be noted again that the MM energies are only semiquantitative because the absolute values calculated with different force field versions are not identical. The tendencies, however, remain the same.[4b] We use force field version A[4b] (soft restraints) for stereoselectivity calculations within one coordination mode and version F[4b] (no restraints) for the comparison of steric energies between all possible coordination modes. We have chosen only the global minimum of each structure, since the local minimum next to the global one does not qualitatively change the energetic order of two *iso*-(*1,2*)-transition state (cf. Scheme 3). In detail, suitable initial structures with ligands **2**−**5** were subject to two 100 ps gas-phase MD simulations at constant high temperature (1000 K), a sampling technique which seems to be sufficient for this type of system. The second simulation was started with the lowest energy structure of the previous run. Every 1 ps the structures were minimized, and the lowest energy structures of both simulations (which have proven to be identical) were taken as global minima. For complexes of ligands **6** and **7**, analogous 200 ps simulations were repeated with the lowest energy structure of the previous run until two subsequent simulations gave the same global minimum.

The calculations of ee's follow the formula (*iso*-(*1,2*)-transition states, $T = 298$ K)

$$\text{ee}\ (\%) = \frac{e^{|E^{\#}_{iso\text{-}1} - E^{\#}_{iso\text{-}2}|/RT} - 1}{e^{|E^{\#}_{iso\text{-}1} - E^{\#}_{iso\text{-}2}|/RT} + 1} \times 100$$

In this formula, changes of temperature have only a small influence.

Results and Discussion

A. Coordination Modes of Monophosphine Ligands. Before the ligands **2**−**7** will come to the fore, we should gain some insight into the electronic factors which control the coordination modes of such phosphine compounds. To this purpose, model systems (two identical monophosphine ligands instead of one chelate) have been calculated by DFT methods. The corresponding reactions—preequilibria of the hydroformylation cycle and olefin insertion as its first step—are depicted in Scheme 2.

The transition states of olefin insertion (**13**) are of early nature and therefore assumed to have an approximately trigonal-bipyramidal geometry.[4,13b] Within this geometry type, an axial−equatorial coordination mode *ae* as well as an equatorial−equatorial coordination mode *ee* are available for two identical monophosphine ligands. The *ae*/*ee* distribution in the precursor complexes of type **11** has been investigated by several authors.[13,24,25] In addition to previous results,[13] we have calculated the whole reaction profile of olefin insertion (substrate = ethylene) for PH_3 and PF_3 (Table 1).

Whereas *ae* and *ee* in complexes **11**−**13** are equally distributed for PH_3, PF_3 leads to a nearly constant *ee* stabilization of about 2 kcal mol^{-1}.[24] In contrast to a previous interpretation,[24] carbonyl dissociation from **11** to **10** is less favorable in the case of PF_3. The experimentally observed increase in activity for ligands of decreasing basicity, i.e., PF_3 vs PH_3,[24,26] may be due to

(12) Godbout, N.; Salahub, D. R.; Andzelm, J.; Wimmer, E. *Can. J. Chem.* **1992**, *70*, 560.
(13) (a) Schmid, R.; Herrmann, W. A.; Frenking, G. *Organometallics* **1997**, *16*, 701. (b) Schmid, R. Ph.D. Thesis, Technische Universität München, München, Germany, 1997.
(14) Ziegler, T. *Chem. Rev.* **1991**, *91*, 651.
(15) (a) Becke, A. *Phys. Rev. A* **1988**, *38*, 3098. (b) Perdew, J. P. *Phys. Rev. B* **1986**, *33*, 8822.
(16) Andzelm, J.; Wimmer, E. *J. Chem. Phys.* **1992**, *96*, 1280.
(17) (a) DGauss 4.0, Oxford Molecular, 1998. (b) UniChem 4.0, Oxford Molecular, 1998.
(18) Frisch, M. J.; Trucks, G. W.; Schlegel, H. B.; Scuseria, G. E.; Robb, M. A.; Cheeseman, J. R.; Zakrzewski, V. G.; Montgomery, J. A., Jr.; Stratmann, R. E.; Burant, J. C.; Dapprich, S.; Millam, J. M.; Daniels, A. D.; Kudin, K. N.; Strain, M. C.; Farkas, O.; Tomasi, J.; Barone, V.; Cossi, M.; Cammi, R.; Mennucci, B.; Pomelli, C.; Adamo, C.; Clifford, S.; Ochterski, J.; Petersson, G. A.; Ayala, P. Y.; Cui, Q.; Morokuma, K.; Malick, D. K.; Rabuck, A. D.; Raghavachari, K.; Foresman, J. B.; Cioslowski, J.; Ortiz, J. V.; Stefanov, B. B.; Liu, G.; Liashenko, A.; Piskorz, P.; Komaromi, I.; Gomperts, R.; Martin, R. L.; Fox, D. J.; Keith, T.; Al-Laham, M. A.; Peng, C. Y.; Nanayakkara, A.; Gonzalez, C.; Challacombe, M.; Gill, P. M. W.; Johnson, B.; Chen, W.; Wong, M. W.; Andres, J. L.; Gonzalez, C.; Head-Gordon, M.; Replogle, E. S.; Pople, J. A. Gaussian 98, Revision A.5; Gaussian Inc., Pittsburgh, PA, 1998.
(19) Casey, C. P.; Whiteker, G. T. *Isr. J. Chem.* **1990**, *30*, 299.
(20) Casey, C. P.; Whiteker, G. T.; Melville, M. G.; Petrovich, L. M.; Gavney, J. A.; Powell, D. R. *J. Am. Chem. Soc.* **1992**, *114*, 5535.
(21) Maple, J. R.; Dinur, U.; Hagler, A. T. *Proc. Natl. Acad. Sci. U.S.A.* **1988**, 5350.
(22) Herrmann, W. A.; Schmid, R.; Kohlpaintner, C. W.; Priermeier, T. *Organometallics* **1995**, *14*, 1961.
(23) (a) Insight/Discover, Release 97.0; MSI, San Diego, CA, 1997. (b) *Discover 95.0/3.0.0 User Guide*; BIOSYM/MSI, San Diego, CA, 1995.
(24) Van der Veen, L. A.; Boele, M. D. K.; Bregman, F. R.; Kamer, P. C. J.; van Leeuwen, P. W. N. M.; Goubitz, K.; Fraanje, J.; Schenk, H.; Bo, C. *J. Am. Chem. Soc.* **1998**, *120*, 11616.
(25) Brown, J. M.; Kent, A. G. *J. Chem. Soc., Perkin Trans. 2* **1987**, 1597.
(26) Tolman, C. A. *Chem. Rev.* **1977**, *77*, 313.

Scheme 2. Preequilibria and Olefin Insertion in the Hydroformylation Cycle

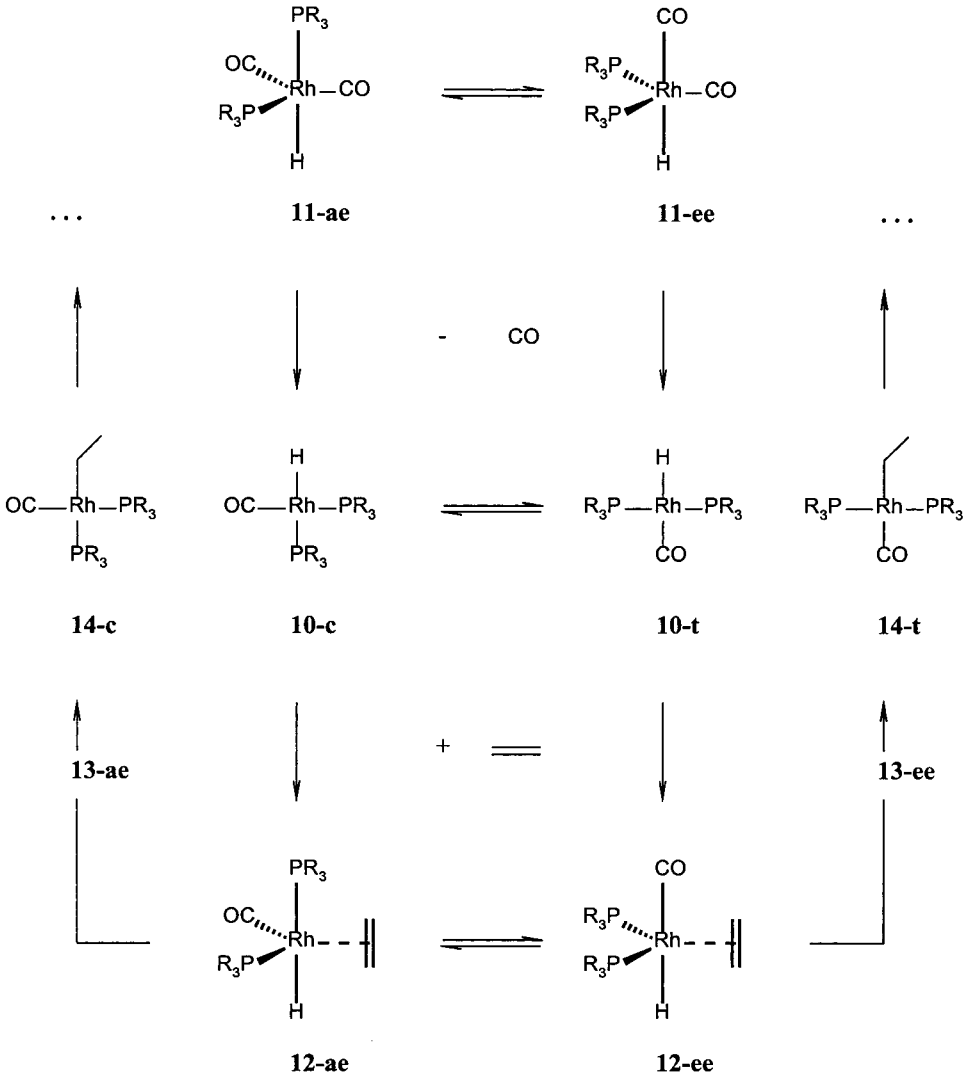

Table 1. Metal Complexes 10−14

complex	E_{PH_3} (kcal mol^{-1})[a]	E_{PF_3} (kcal mol^{-1})[a]
11-ae	−22.7	−24.6[b]
11-ee	−22.9	−27.0
10-c	+1.4[b]	+0.9[b]
10-t	0	0
12-ae	−12.0	−17.7
12-ee	−12.3	−20.3
13-ae	+1.9	−10.9
13-ee	+1.6	−12.4
14-c	−13.3	−18.0
14-t	−15.6	−19.5[b]

[a] Relative NLDA energies including zero-point correction (program Gaussian98; see Computational Methods). [b] Optimized geometry with negligible imaginary frequencies.

the greater stability of the alkene complexes **12** (∼6 kcal mol^{-1}) and the halved barrier for olefin insertion (7 vs 14 kcal mol^{-1}).[27] We have also calculated the *cis*/*trans* distribution[28] in the square-planar rhodium complexes **10** with phosphine ligands of variable electronic and steric properties[26,29] (Table 2).

Table 2. Metal Complexes 10-(c,t)

R	$E_{\mathbf{10\text{-}c}}$ (kcal mol^{-1})[a]	$E_{\mathbf{10\text{-}t}}$ (kcal mol^{-1})[a]
H	2.2 (2.4)	0
F	1.6 (1.4)	0
Me	4.3 (2.6)	0
R_1 = Me, R_2 = R_3 = Ph	5.4 (0)[b,c]	0 (2.7)[b,c]

[a] Relative NLDA energies without zero-point correction. LDA energies are given in parentheses (program DGauss, see Computational Methods). [b] NLDA single-point energies (see Computational Methods). [c] No frequency calculation.

10-c opens the insertion pathway with coordination mode *ae* and is less stable than **10-t** for PH_3 as well as PF_3. The energetic spacing decreases from PH_3 to PF_3 and can be identically described by LDA and NLDA calculations. In the case of $PMePh_2$ (the most suitable electronic model for ligands **2** and **4**−**7**) and PMe_3, which are more basic than PH_3,[24,26] electronic and steric effects are mixed. The LDA energies of **10-c** are significantly lower than the NLDA values. For $PMePh_2$, **10-c** is more stable than **10-t** on the LDA level. It must be kept in mind that LDA overestimates and NLDA underesti-

(27) Gleich, D.; Herrmann, W. A. Manuscript in preparation.
(28) In the case of isomers, LDA energies are already sufficient.[14]
(29) González-Blanco, Ò.; Branchadell, V. *Organometallics* **1997**, *16*, 5556.

Scheme 3. Coordination Modes and Transition States with C_2-Symmetric Bisphosphine Ligands

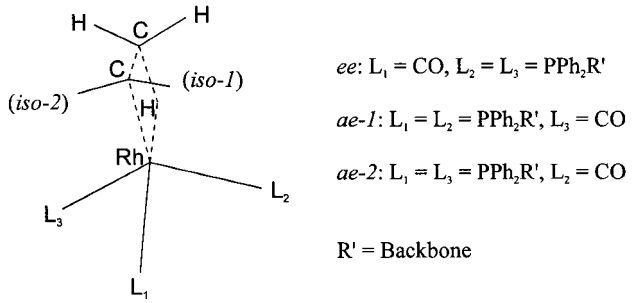

mates nonbonding interactions which are crucial for $PMePh_2$ because of π-stacking effects.[13,14,30,31] Therefore, apart from computational costs, pure DFT calculations are no method of choice to judge the coordination preferences of "real" phosphine ligands. The calculation of styrene stereoselectivities is treacherous, also. This methodical conclusion is another backing for a combined QM/MM treatment.[4,13b] The summarized chemical conclusion is that the electronic *ae*/*ee* gap in the transition states of olefin insertion **13** is narrow: less basic phosphine ligands (e.g., PF_3) slightly favor the coordination mode *ee*, more basic phosphine ligands such as PH_3 have no pronounced preference, and those with phenyl substituents (e.g., $PMePh_2$) presumably tend to *ae*.

B. Coordination Modes of C_2-Symmetric Bisphosphine Ligands and Consequences for the Stereoselectivity. C_2-Symmetric bisphosphine ligands generally allow one chelation possibility and two *iso*-transition states for each coordination mode depicted in Scheme 3.

All coordination modes contribute with their individual asymmetric induction to the total stereoselectivity. To achieve high ee's, at least one of the following requirements should be met.

(i) *One* coordination mode is significantly stabilized, i.e., (a) *ee* vs *ae*-(*1,2*) or (b) *ae-1* vs *ae-2* (requirement of preferred asymmetric induction, RPAI). With regard to the results of section A, steric factors play a key role in case a, viz., PBA (preferred bite angle, see Computational Methods) and ligand flexibility (cf. section D).[4b,24] Especially in case b, solvent effects may be decisive (cf. section C), which lies beyond the range of our model and also far away from a comprehensible treatment.

(ii) *All* coordination modes favor transition states with the *same* asymmetric induction (requirement of synchronous asymmetric inductions, RSAI). This requirement is more reliable, for the energetic order of different coordination modes is less relevant now while different transition states of one coordination mode can be reasonably described in the gas phase.[4b] If only *ae-1* and *ae-2* are available, the transition states of an achiral ligand such as DIPHOS (**8**) are mutually enantiomeric, which is equivalent to exactly *opposite* asymmetric inductions and a cancellation of stereoselectivities, respectively (Scheme 4).

Therefore, a chiral ligand has to compensate for this "natural" cancellation by suitable backbone interactions, as is demonstrated by BINAPHOS (**1**).[4a] When *ee* is available, also, the situation becomes even more demanding. In both cases, the ligand performance is rated in the same manner: synchronous asymmetric inductions stand for high total stereoselectivity, whereas any antagonism should damage the stereodifferentiation, provided that the RPAI is not met strongly.

Scheme 4. Cancellation of Stereoselectivities in the Case of an Achiral Ligand

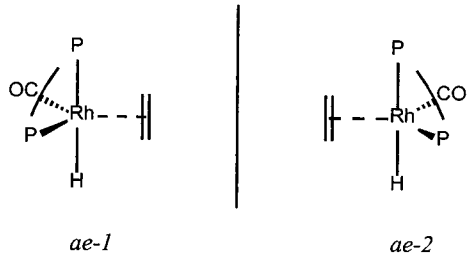

ae-1 *ae-2*

Table 3. Metal−Ligand Fragments with 2 and 3 (PBA Simulations)

ligand	N_R[a]	PBA (deg)[b]	bite-angle range (deg)[c]	energy range (kcal mol^{-1})[d]	N_S[e]
CHIRAPHOS (**2-(*S,S*)**)	5	79.6	79.0−80.8	1.5	4
BINAP (**3-(*R*)**)	7	90.0	90.0−90.8	0.3	2

[a] Number of ring members. [b] Preferred bite angle (see Computational Methods). [c] Bite-angle range of all stable structures (see Computational Methods). [d] Energy range of all stable structures (see Computational Methods). [e] Number of all stable structures (see Computational Methods).

Table 4. Coordination Modes and Transition States with 2 and 3 (Substrate Styrene)

ligand	CM[a]	TS[a]	$E^{\#}$ (kcal mol^{-1})[b]	ee (%)[c] [confign]	ee (%) [confign]
CHIRAPHOS (**2-(*S,S*)**)	*ae-1*	*iso-1*	1.9	92 [*S*]	24 [*R*][d]
		iso-2	0 (1.1)		
	ae-2	*iso-1*	0 (0)	99 [*R*]	
		iso-2	3.4		
BINAP (**3-(*R*)**)	*ae-1*	*iso-1*	0.7	53 [*S*]	
		iso-2	0 (1.1)		
	ae-2	*iso-1*	0 (0)	>99 [*R*]	
		iso-2	4.0		

[a] Coordination modes and transition states, respectively (cf. Scheme 2). [b] Relative transition-state energies. Relative energies of the coordination modes are given in parentheses (see Computational Methods). [c] Calculated ee's (see Computational Methods). [d] Experimental ee.[32]

C. C_2-Symmetric Bisphosphine Ligands with Coordination Modes *ae*-(*1,2*). CHIRAPHOS (**2**) and BINAP (**3**) are very rigid ligands with clearly axial−equatorial coordination preferences, as can be seen from qualitative considerations and bite-angle calculations (Table 3). The PBA of **2** is smaller than the PBA of **3**, but the bite-angle range as well as the number of stable structures (N_S) indicate that, despite its larger size, the BINAP chelate ring is stiffer than the CHIRAPHOS ring.

The transition-state energies and corresponding stereoselectivities of *ae*-(*1,2*) are listed in Table 4. The geometries of the energetically favored transition states are depicted in Figures 1 and 2.

The qualitative distribution of transition-state energies is the same for **2** and **3** and follows from the minor steric demand of the carbonyl group: analogous to DIPHOS (**8**) (cf. Chart 1), *ae-1*/*iso-2* and *ae-2*/*iso-1* are favored. The energetic order of the two coordination

(30) Becke, A. *J. Chem. Phys.* **1993**, *98*, 1372.
(31) Pietsch, M. A.; Rappé, A. K. *J. Am. Chem. Soc.* **1996**, *118*, 10908.

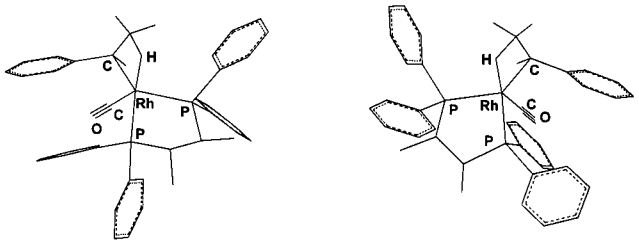

2/*ae-1*/*iso-2* **2**/*ae-2*/*iso-1*

Figure 1. Calculated geometries of the energetically favored transition states for CHIRAPHOS (**2**) (substrate styrene). For clarity, hydrogen atoms of the ligand as well as of the styrene phenyl ring are omitted; all atoms marking the approximately trigonal-bipyramidal geometries of the transition states are labeled.

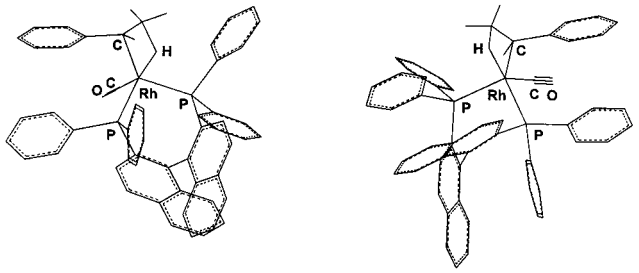

3/*ae-1*/*iso-2* **3**/*ae-2*/*iso-1*

Figure 2. Calculated geometries of the energetically favored transition states for BINAP (**3**) (substrate styrene). For clarity, hydrogen atoms of the ligand as well as of the styrene phenyl ring are omitted; all atoms marking the approximately trigonal-bipyramidal geometries of the transition states are labeled.

modes is also identical: *ae-2* < *ae-1* (~1 kcal mol^{-1}). It is, however, impossible to decide from the calculations how *ae-1* and *ae-2* are exactly distributed because solvent effects may invert this small difference.

Since the RSAI is not met for either ligand, the total stereoselectivity should be rather low. In the case of CHIRAPHOS (**2**), a direct comparison with experimental rhodium/styrene results confirms this conclusion (Table 4).[32] The predominant contribution for the total stereoselectivity is assigned to *ae-2*, which also agrees with the theoretical results. In the case of BINAP (**3**), we were not able to find experimental results for styrene. The quantitative energy distribution suggests a stronger chiral induction of **3**, for the ee of *ae-2* is significantly higher than that of *ae-1*. The hydroformylation of functionalized olefins gives 7% ee for methyl *N*-acetamidoacrylate and 47% ee for vinyl acetate.[33,34] However, the message of these values is restricted, since the heteroatoms of such olefins can coordinate to the metal atom, thus shifting the regioselectivity toward the *iso*-aldehydes.[33] The two assumptions of our model mentioned in the Introduction may then no longer be acceptable. A further comparison with experimental platinum/styrene results exhibits enhanced stereoselectivities (45% ee (*R*) for CHIRAPHOS[32] and 69% ee

Table 5. Minimized Metal−Ligand Fragments of Transition States with 2 and 3

ligand	CM[a]	TS[a]	*E* (kcal mol^{-1})[b]	bite angle (deg)[c]	sym
CHIRAPHOS (**2-(*S,S*)**)	*ae-1*	*iso-1*	0	79.6	C_1
		iso-2	0	79.6	C_1
	ae-2	*iso-1*	0	79.6	C_1
		iso-2	0	79.6	C_1
BINAP (**3-(*R*)**)	*ae-1*	*iso-1*	0	90.0	C_2
		iso-2	0.3	90.8	C_1
	ae-2	*iso-1*	0.3	90.8	C_1
		iso-2	0.3	90.8	C_1

[a] Coordination modes and transition states, respectively (cf. Scheme 2). [b] Energies of the minimized metal−ligand fragments relative to the global minima of the PBA simulations (cf. Table 3). [c] Bite angle (cf. Table 3).

Table 6. Metal−Ligand Fragments with 4 and 5 (PBA Simulations)

ligand	N_R[a]	PBA (deg)[b]	bite-angle range (deg)[c]	energy range (kcal mol^{-1})[d]	N_S[e]
DIOP (**4-(*R,R*)**)	7	102.4	94.8−123.1	4.1	>5
NAPHOS (**5-(*R*)**)	9	118.5	102.6−132.2	8.1	>5

[a] Number of ring members. [b] Preferred bite angle (see Computational Methods). [c] Bite angle range of all stable structures (see Computational Methods). [d] Energy range of all stable structures (see Computational Methods). [e] Number of all stable structures (see Computational Methods).

(*R*) for BINAP[35]). The BINAP/platinum experiments give one example of inversion in product chirality with increasing temperature. This phenomenon can be explained (i) by kinetic reasons (i.e., the RPAI is met, cf. section B) or (ii) by free rotation of one phenyl group (i.e., thermal motion).[3] One hint that (i) is operative is obtained if one minimizes the isolated metal−ligand fragment geometry of each transition state analogous to the PBA optimization (Table 5). The CHIRAPHOS fragment relaxes to the global C_1-symmetric minimum (cf. Table 3), whereas the BINAP fragment takes the global C_2-symmetric minimum only for *ae-1*/*iso-1*. In all other cases, C_2 symmetry is broken by rotation of one phenyl group.

Therefore, phenyl rotation seems to be also an intrinsically steric effect in the case of substrate coordination.

D. C_2-Symmetric Bisphosphine Ligands with Coordination Modes *ae*-(*1,2*) and *ee*. DIOP (**4**) and NAPHOS (**5**) offer chelating properties different from those of CHIRAPHOS (**2**) and BINAP (**3**) (cf. Table 3), since the bite angle covers a wider range (30 vs 1°) and more stable fragments are possible (Table 6). A comparison of DIOP and BINAP parameters shows that the number of ring members (N_R) alone poorly describes the ligand characteristics.

The transition-state energies and corresponding stereoselectivities of *ee* and *ae*-(*1,2*) are listed in Table 7. The geometries of *ee*/*iso*-(*1,2*) and the energetically favored *ae*-(*1,2*) transition states are depicted in Figures 3 and 4.

The qualitative distributions of transition-state energies are not the same for **4** and **5** and differ from those of **2** and **3**, which is a consequence of the much greater backbone flexibilities. For **4**/*ee*, the energetic spacing between *iso-1* and *iso-2* is directly caused by the arrangement of the phenyl groups, since the backbone

(32) Consiglio, G.; Morandini, F.; Scalone, M.; Pino, P. *J. Organomet. Chem.* **1985**, *279*, 193.
(33) Gladiali, S.; Pinna, L. *Tetrahedron: Asymmetry* **1990**, *1*, 693.
(34) Sakai, N.; Nozaki, K.; Mashima, K.; Takaya, H. *Tetrahedron: Asymmetry* **1992**, *3*, 583.
(35) Kollar, L.; Sandor, P. Szalontai, G. *J. Mol. Catal.* **1991**, *67*, 191.

Table 7. Coordination Modes and Transition States with 4 and 5 (Substrate Styrene)

ligand	CM[a]	TS[a]	$E^{\#}$ (kcal mol^{-1})[b]	ee (%)[c] [confign]	ee (%) [confign]
DIOP (**4-(*R,R*)**)	*ee*	*iso-1*	1.6	87 [*S*]	10 [*R*][d]
		iso-2	0 (0.3)		
	ae-1	*iso-1*	0 (0)	25 [*R*]	
		iso-2	0.3		
	ae-2	*iso-1*	0.3	25 [*S*]	
		iso-2	0 (1.5)		
NAPHOS (**5-(*R*)**)	*ee*	*iso-1*	0 (0)	59 [*R*]	34 [*S*][e]
		iso-2	0.8		
	ae-1	*iso-1*	1.0	69 [*S*]	
		iso-2	0 (4.8)		
	ae-2	*iso-1*	2.0	95 [*S*]	
		iso-2	0 (3.2)		

[a] Coordination modes and transition states, respectively (cf. Scheme 2). [b] Relative transition-state energies. Relative energies of the coordination modes are given in parentheses (see Computational Methods). [c] Calculated ee's (see Computational Methods). [d] Experimental ee.[32] [e] Experimental ee.[38]

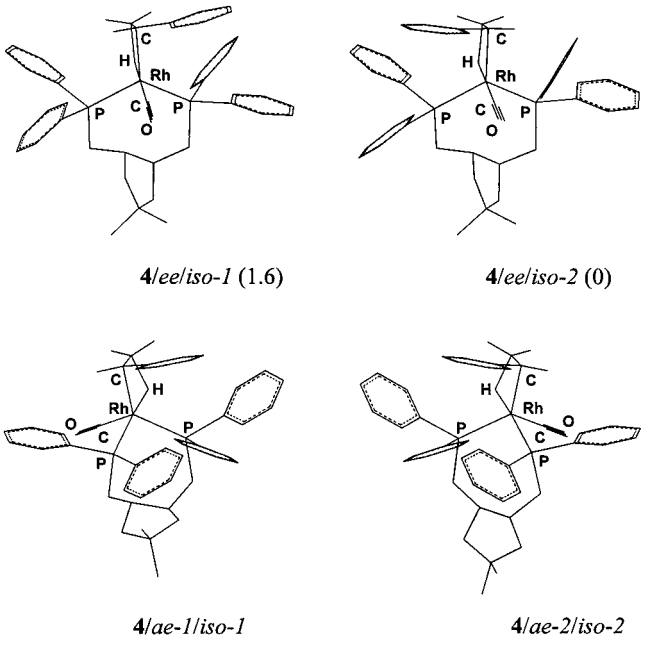

Figure 3. Calculated geometries of *ee*/*iso*-(*1,2*) and the energetically favored *ae*-(*1,2*) transition states for DIOP (**4**) (substrate styrene). For clarity, hydrogen atoms of the ligand as well as of the styrene phenyl ring are omitted; all atoms marking the approximately trigonal-bipyramidal geometries of the transition states are labeled. Relative energies $E^{\#}$ (kcal mol^{-1}) are given in parentheses.

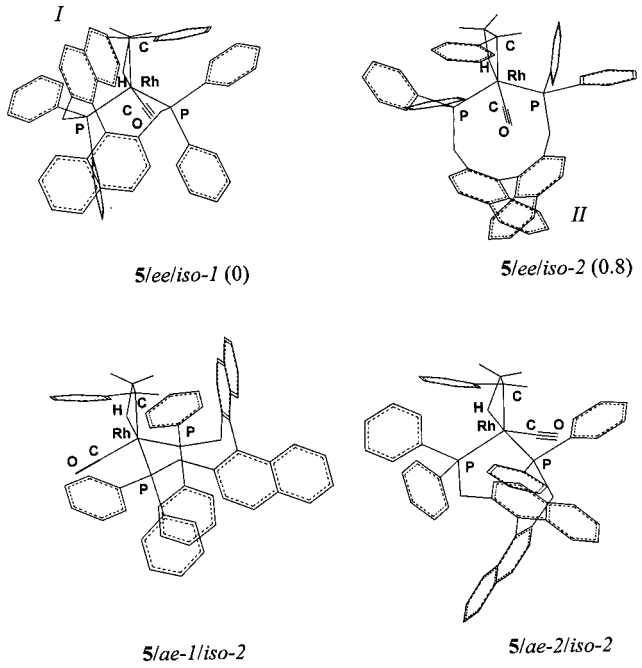

Figure 4. Calculated geometries of *ee*/*iso*-(*1,2*) and the energetically favored *ae*-(*1,2*) transition states for NAPHOS (**5**) (substrate styrene). For clarity, hydrogen atoms of the ligand as well as of the styrene phenyl ring are omitted; all atoms marking the approximately trigonal-bipyramidal geometries of the transition states are labeled. Relative energies $E^{\#}$ (kcal mol^{-1}) are given in parentheses.

Table 8. Minimized Metal−Ligand Fragments of Transition States with 4 and 5[a]

ligand	CM[b]	TS[b]	E (kcal mol^{-1})[c]	bite angle (deg)[d]
DIOP (**4-(*R,R*)**)	*ee*	*iso-1*	1.5	123.1
		iso-2	1.5	123.1
	ae-1	*iso-1*	0	102.4
		iso-2	0	102.4
	ae-2	*iso-1*	0.3	100.8
		iso-2	1.9	101.7
NAPHOS (**5-(*R*)**)	*ee*	*iso-1*	4.1	118.7
		iso-2	5.4	120.4
	ae-1	*iso-1*	4.1	118.7
		iso-2	6.2	113.2
	ae-2	*iso-1*	4.1	118.7
		iso-2	4.1	118.7

[a] The symmetry for each fragment is C_1. [b] Coordination modes and transition states, respectively (cf. Scheme 2). [c] Energies of the minimized metal−ligand fragments relative to the global minima of the PBA simulations (cf. Table 6). [d] Bite angle (cf. Table 6).

conformation remains the same (Figure 3). For **5**/*ee*, two quite dissimilar backbone conformations *I*/*II* analogous to BISBI[4b] (**9**) (cf. Chart 1) rule the energetic order of *iso-1*/*iso-2* (Figure 4). In the case of **4**/*ae-(1,2)*, the asymmetric inductions of the favored transition states are in contrast to those in section C; i.e., the influence of the ligand backbone is now important. The influence of the chirality centers is less important: after reflection, the arrangement of the phenyl groups and the ring conformation are the same for both transition states (Figure 3). Hence, the induction preferences are opposite and, beyond that, the stereoselectivities of both coordination modes are low. On the other hand, the axial chirality of **5** leads to a larger discrimination between *ae-1* and *ae-2* that can be seen from variable backbone conformations (Figure 4) as well as from the higher energetic spacing between *iso-1* and *iso-2* and the synchronous asymmetric inductions. The energetic order of the coordination modes of **4** is *ae-1* < *ee* < *ae-2* (maximum 1.5 kcal mol^{-1}), fitting the results of both PBA simulation (cf. Table 6) and experiment (see below).[36] In contrast, the **5**/*ae*-(*1,2*) transition states are of significantly higher steric energy than the *ee* ones (∼4 kcal mol^{-1}).[37] Yet, according to the minimized metal−ligand fragment geometries of each transition state (cf. section C), there exists no major hindrance for axial−equatorial coordination (Table 8): Whereas the DIOP fragments of *ee* and *ae*-(*1,2*), respectively, relax to minima with two distinct angle sizes (approximately 120 and 100°, respectively), the four NAPHOS fragments of

(36) With regard to the results of section A, only the steric energy is considered (see also Computational Methods).

(37) The differences are similar to those of BISBI (**9**)/propene transition states.[4b]

Table 9. Coordination Modes and Transition States with 6 and 7 (Substrate Styrene)

ligand	CM[a]	TS[a]	BC[b]	$E^{\#}$ (kcal mol^{-1})[c]	ee (%)[d] [confign]
6-(*R*)	*ee*	*iso-1*	*I*	0	80 [*R*]
		iso-2	*II*	1.3	
	ae-1	*iso-1*	*II*	1.2	77 [*S*]
		iso-2	*I*	0	
	ae-2	*iso-1*	*II*	2.2	95 [*S*]
		iso-2	*II*	0	
7-(*R*)	*ee*	*iso-1*	*II*	0	53 [*R*]
		iso-2	*II*	0.7	
	ae-1	*iso-1*	*II*	0	97 [*R*]
		iso-2	*II*	2.5	
	ae-2	*iso-1*	*I*	0	>99 [*R*]
		iso-2	*II*	3.7	

[a] Coordination modes and transition states, respectively (cf. Scheme 2). [b] Backbone conformations (cf. Figure 4). [c] Relative transition-state energies (see Computational Methods). [d] Calculated ee's (see Computational Methods).

ee/*iso-1*, *ae-1*/*iso-1*, and *ae-2*/*iso-*(*1,2*) belong to the same local minimum (118.7°). The energetic difference of 4.1 kcal mol^{-1} to the global minimum of the PBA simulation (cf. Table 6), in conjunction with similar bite angles (118.7 vs 118.5°), points to the limitations of the natural bite angle concept[19,20] for large and flexible rings.

Again, the RSAI is not met for either ligand, which suggests that the total stereoselectivity should be rather low. A direct comparison with experimental rhodium/styrene results[32,38] confirms this conclusion (Table 7). The predominant contribution for the total stereoselectivity is assigned to **4**/*ae-1* and **5**/*ae-*(*1,2*); the selectivity ranking is **4** < **5**. A further comparison with experimental platinum/styrene results exhibits inverted stereoselectivities for **4** (4% ee (*S*)[32]). Especially for the **5**/rhodium system, these values are indicative of the RPAI (cf. section B) and make evident the limitations of our method. Nevertheless, its predictive potential will be demonstrated in the next section.

E. New C_2-Symmetric Bisphosphine Ligands Derived from NAPHOS (5). Since **5** is the most versatile of the C_2-symmetric ligands in terms of both flexibility and selectivity, we now investigate its derivatives **6** and **7** (Chart 1) without experimental background. The transition-state energies and corresponding stereoselectivities of *ee* and *ae-*(*1,2*) are listed in Table 9.[39]

All six transition-state geometries of **6** are identical with those of **5**. This identity also applies to the energetic order (cf. Table 7). Therefore, the RSAI is not met once again. As a consequence of the 2-substitution, the naphthyl−phosphorus units of **6** shield the reaction center in a manner similar to that for the phenyl rings of **5.**

In contrast to **6**, only three transition-state geometries of **7**, viz., *ee*/*iso-2*, *ae-1*/*iso-1*, and *ae-2*/*iso-2*, are approximately identical with those of **5**. The energetic order is different from **5** as well as from **6**. **7** fulfills the RSAI−theory predicts a highly selective ligand in front of experiment. As a consequence of the 1-substitution, the naphthyl−phosphorus units of **7** shield the reaction center more effectively than the phenyl rings of **5**. The decisive improvement upon **5**, i.e., elimination of the induction fissure between *ee* and *ae-*(*1,2*), is assisted by suitable interchanges of the backbone conformations *I* and *II* (cf. Figure 4). Unfortunately, this specific solution cannot be extended to a general principle. Apart from that, the activity might be low, owing to the considerable steric demand of the naphthyl rings. Experimental tests in our laboratory will clarify the performance of **7**.

Concluding Remarks

Based on the RSAI (requirement of synchronous asymmetric inductions), which states that all ligand coordination modes favor transition states with the same asymmetric induction, the performance of C_2-symmetric bidentate phosphine ligands in asymmetric hydroformylation is governed by two interdependencies.

(i) The smaller the chelate ring (e.g., in the case of CHIRAPHOS (**2**) and BINAP (**3**)), the more diminished its influence on asymmetric induction for the only available axial−equatorial coordination modes *ae-*(*1,2*); i.e., the "natural" cancellation of stereoselectivities cannot be overcome.

(ii) A larger chelate ring often entails a greater backbone flexibility (e.g., in the case of DIOP (**4**) and NAPHOS (**5**)), and the equatorial−equatorial coordination mode *ee* must be additionally considered. This promotes antagonisms that should again impair the total stereoselectivity. The promising new ligand **7** seems to be a random exception.

Generally, C_2-symmetric ligands offer the evident advantage of only one chelation possibility per coordination mode and the inherent disadvantage of minor stereodifferentiation: the outstanding quality of the C_1-symmetric ligand BINAPHOS (**1**) is not only a consequence of reduced coordination modes and chelation possibilities but also of the right number and configuration of chirality centers.[4a,7] However, C_1 symmetry alone is just as poor a cure-all as the accumulation of chirality centers: **2** has two stereocenters and only the coordination modes *ae-*(*1,2*) but low stereoselectivity, whereas **7** has only one stereocenter and additionally the coordination mode *ee* but is expected to be highly selective.

Our explanations and predictions release asymmetric hydroformylation from its predominantly empirical character, although the magic formula for ligand development is still unknown.

Acknowledgment. This work was generously supported by the Deutsche Forschungsgemeinschaft and the Fonds der Chemischen Industrie. We thank the John von Neumann Institute for Computing, Jülich, Germany, for excellent service as well as our hydroformylation experts F. Rampf and R. Eckl for helpful discussions.

Supporting Information Available: Tables giving coordinates and absolute energies of all transition states for **2**−**7**. This material is available free of charge via the Internet at http://pubs.acs.org.

OM990393E

(38) Eckl, R. W.; Priermeier, T.; Herrmann, W. A. *J. Organomet. Chem.* **1995**, *532*, 243.

(39) The energetic order of the coordination modes of both ligands is similar to that of **4** (cf. Table 7).